

### **NPL REPORT TQE 33**

**An Algorithm for Fitting Q-factor to Scalar Transmission-Coefficient Data with Asymmetric Peak** 

**A P Gregory** 

**MAY 2025** 

# An Algorithm for Fitting Q-factor to Scalar Transmission-Coefficient Data with Asymmetric Peak

### A. P. Gregory

Electromagnetic Technologies Group
Electromagnetic and Electrochemical Technologies Department

#### **ABSTRACT**

This report presents an algorithm for obtaining Q-factor by fitting to swept-frequency scalar measurements on resonances that are asymmetric as a result of a leakage signal. Formulae for obtaining estimates of the unloaded Q-factor are also derived. Comparisons are made between Q-factors fitted by scalar and vector algorithms to measured data, and to simulated data. Example computer-codes and test examples are given.

© NPL Management Limited, 2025

ISSN 1754-2995

https://doi.org/10.47120/npl.TQE33

National Physical Laboratory Hampton Road, Teddington, Middlesex, TW11 0LW

This report is licensed under the Creative Commons CC-BY-ND 3.0 Licence. The full legal code is available at https://creativecommons.org/licenses/by-nd/3.0/.

The Computer Source Code Listings that are included in the report are licensed under the Creative Commons CC0 1.0 Public Domain Dedication.

The full legal code is available at https://creativecommons.org/publicdomain/zero/1.0/.

Approved on behalf of NPLML by Tian Hong Loh,
Science Area Leader

# **CONTENTS**

### **ABSTRACT**

1	INTRODUCTION	1
	1.1 ASYMMETRIC RESONANT PEAKS	2
	1.2 PREVIOUS WORK	2
2	SPECIFICATION	4
3	THEORY	5
4	ROBINSON & CLEGG'S 3-COEFFICIENT SOLUTION	6
5	ITERATIVE 5-COEFFICIENT SOLUTION	8
6	ESTIMATION OF UNLOADED Q-FACTOR	12
7	TESTS	14
	7.1 TEST 1: FITTING-METHOD COMPARISON FOR WELL-SHAPED EXPERIMENTAL DATA	14
	7.2 TEST 2: COMPARISON OF VECTOR AND SCALAR FITS TO SIMULATED DATA WITH NOISE BUT NO LEAKAGE	
	7.3 TEST 3: CALCULATIONS OF UNLOADED Q-FACTOR WHEN THERE IS LEAKAGE	19
8	CONCLUSION	20
Di	EEEDENICES	21

# **TABLES**

Table 1:	Q-factor fitting methods that are investigated	14
Table 2:	Vector and scalar fits for a measurement on a Split-Post Dielectric Resonator (SPDR)	14
Table 3:	Results of simulations for a resonance with noise but no leakage $\ \ \ldots \ \ \ldots$	19
Table 4:	Unloaded Q-factors obtained from the coefficients fitted by SCALARFIT5 by using equations (26) and (27)	19

# **FIGURES**

Figure 1:	Example measurement on a cavity resonator
Figure 2:	Polar and magnitude plots of transmission ( $S_{21}$ ) at resonance $\ldots \ldots$ 3
Figure 3:	Fitted resonance of a Split-Post Dielectric Resonator
Figure 4:	Simulated data with VNA receiver noise
Figure 5:	Simulations of Q-factors fitted by Robinson and Clegg's algorithm 18
Figure 6:	Simulated resonances with leakage signal

# **CODE LISTINGS**

Listing 1:	Robinson and Clegg's method of solution
Listing 2:	Obtain all five initial values for iterative solution
Listing 3:	: Iterative solution by using a library function
Listing 4:	: Function for calculating the Jacobian matrix
Listing 5:	: Function for calculating the residual error
Listing 6:	: Calculation of unloaded Q-factor
Listing 7:	Function for generating trial $S_{21}$ data with VNA receiver noise $\ldots \ldots 16$

#### 1 INTRODUCTION

The shapes of the electromagnetic resonances of cavities and LC circuits can be "probed" by using a swept-frequency source and a detection system that measures transmitted amplitude or power via a pair of couplings (Figure 1). Q-factor and resonant frequency can then be obtained by various methods, including a number of fitting algorithms. A previous NPL Report [1] and a paper [2] describe how Q-factor can be obtained by fitting from vector data obtained by using a Vector Network Analyser (VNA) — a combined swept-frequency source and detection system for measuring complex scattering (S-)parameters. Vector methods are more informative and often more accurate than scalar methods but are not always possible, so scalar methods – the subject of this report – are still needed.

In the simplest case, scalar transmission measurements on resonances are Lorentzians for which there are straightforward published methods for fitting Q-factor [3]. The purpose of this report is to present an algorithm for characterising resonances that appear to have asymmetric peaks as a result of an interfering leakage signal that bypasses the resonator. It was developed for obtaining Q-factor at terahertz frequencies from measurements made by using instrumentation based on frequency combs [4] (for which phase data is not available), but it can be applied more generally to measurements on resonators made with spectrum analysers, scalar network analysers and VNAs if scalar output ( $|S_{21}|$ ) is selected.

This report also considers the topic of loading by the measuring instrument. The loaded (measured) Q-factor is referred to as  $Q_L$  and the unloaded Q-factor as  $Q_o$ . Microwave instruments such as VNAs typically have low impedance ports (e.g.  $50\,\Omega$ ), which means that  $Q_L$  is significantly smaller than  $Q_o$  if strong coupling is used.  $Q_o$  cannot be measured directly but, if the measured data is calibrated (or normalised in an uncalibrated system), it can be estimated. When there is a leakage signal,  $Q_o$  is found to have two possible solutions for scalar measurements.

Practical advice on measurement techniques and example computer code (Python<sup>2</sup> with numpy and scipy packages installed) are provided. Q-factor measurements obtained by using scalar-fitting and vector-fitting techniques are also presented.

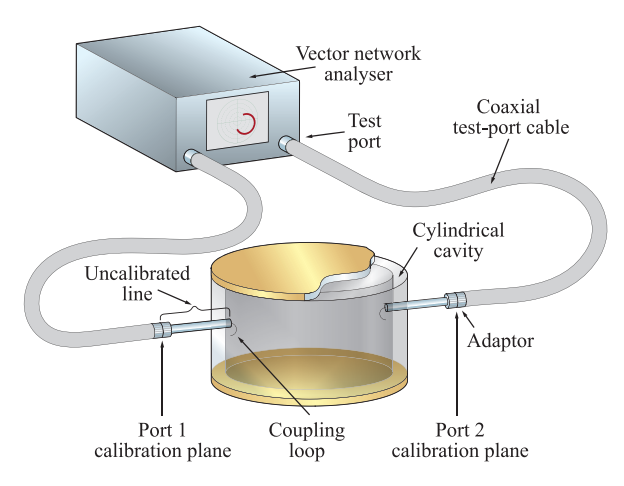


Figure 1: Example measurement on a cavity resonator (from reference [1])...

<sup>&</sup>lt;sup>1</sup> The "power" is actually the relative power in most cases, although some instruments allow absolute power in Watts to be measured.

<sup>&</sup>lt;sup>2</sup> Python Software Foundation, https://www.python.org

#### 1.1 ASYMMETRIC RESONANT PEAKS

On a polar chart (Figure 2), vector  $S_{21}$  data for swept resonances appear as circular arcs (known as Q-circles). These can become distorted if long connecting-cables are used [1], but this has no effect on scalar measurements. At the *pole* of the Q-circle, corresponding to frequency  $\pm \infty$ , no energy is coupled via the resonance. In any practical experiment, however, the pole of the Q-circle is displaced from the centre of the polar chart because of leakage (although this may be very small). Leakage has the effect of making the scalar magnitude (or power) peak asymmetric, which causes error in measurements by the "3 dB point" method as shown in Figure 2. For scalar measurements, noise gives rise to the *noise floor* — a minimum signal level not predicted by Lorentzian models for resonances.

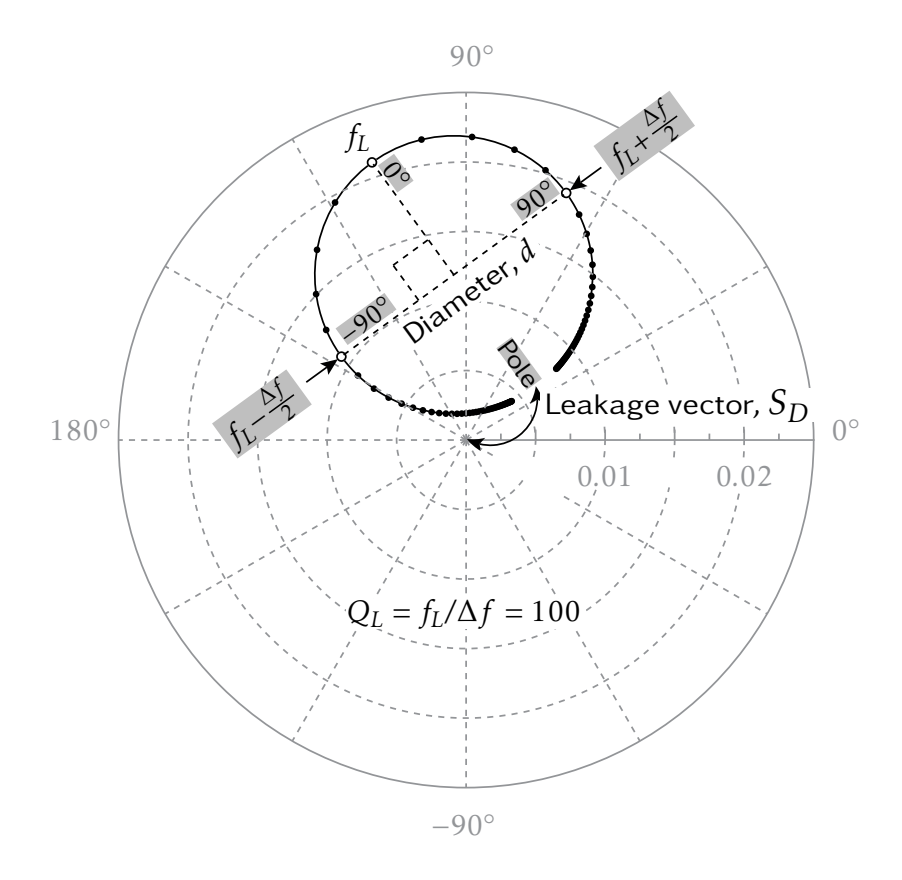
Model equations that describe measurements on resonances with a leakage signal that does not vary in the measured frequency range require five coefficients for scalar fitting, and six coefficients for vector fitting. As the number of fitted coefficients is large, iterative methods (Section 5) of fitting require reasonably accurate initial values for the iteration, otherwise a local minimum that is far from the expected solution may be obtained. For vector measurements, initial values that have high accuracy even when there is significant leakage are readily calculated [1, 2]. This is not necessarily true for convenient methods for obtaining initial values from scalar data because these do not account for asymmetry. Finding initial values that enable a reliable iterative solution is an important aspect of the scalar algorithm described in this report.

#### 1.2 PREVIOUS WORK

Many publications describe equivalent-circuit models for resonators (the book by Pozar [5] is recommended). An overview of methods for obtaining Q-factor from resonance data is given in a previous NPL Report MAT 58 [1], which also presents algorithms for fitting to vector data. Additional examples of vector fitting are provided by reference [2]. The website for the LMFIT Python package [6] provides code examples for fitting scalar models of peaks of various shapes, including Lorentzians, to data. Robinson & Clegg [3] calculate the Q-factor and resonant frequency of a Lorentzian peak from the coefficients of a fitted polynomial. The simplest technique for measuring the Q-factor of Lorentzian peaks uses readout from the cursor facility of instruments such as VNAs and spectrum analysers (see Bray & Roy [7]). The "3 dB points" are often chosen for convenience.

The five coefficients fitted to asymmetric peaks by the scalar algorithm given in this report are the peak power, resonant frequency  $(f_L)$ , loaded Q-factor  $(Q_L)$  and two additional coefficients that characterise the effect of leakage (which is assumed not to vary with frequency). Other workers have used scalar model equations that also include a leakage term that varies linearly with frequency (increasing the number of coefficients in the model equation to six). These include Petersan & Anlage [8], Zadler et al [9], and Kuptsov et al [10].

NPL Report MAT 58 [1] contains extensive background information on techniques for measuring Q-factor by using VNAs. Of particular relevance, it is demonstrated that  $Q_L$  for two-port resonators with weak coupling can be measured by using uncalibrated VNAs without significant loss of accuracy. Moreover, for weak coupling it can often be assumed that  $Q_o \approx Q_L$ . Where needed, there are more rigorous procedures for estimating  $Q_o$  in calibrated and uncalibrated systems. These can be adapted for scalar measurements (Section 6).



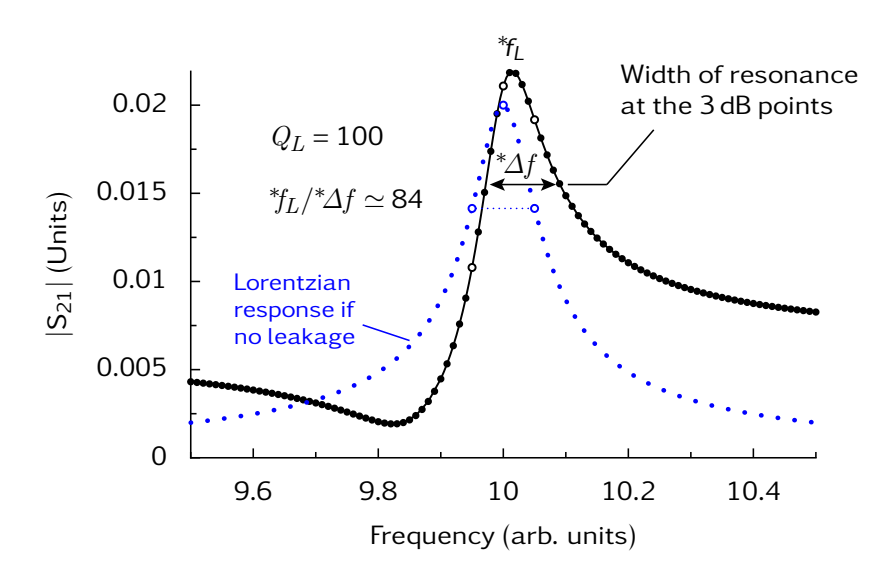


**Figure 2:** Polar (top) and magnitude vs frequency plots of transmission ( $S_{21}$ ) at resonance. The resonant frequency and width obtained by the "3 dB points" method are marked with asterisks on the magnitude plot. These show that the "3 dB point" method of measuring of Q-factor is not accurate when there is significant leakage. The -90°, 0° and 90° points are identified with open circles.

#### 2 SPECIFICATION

When fitting to asymmetric peaks by using the scalar algorithm described in this report, bear in mind the following:

- It is assumed that there may be unwanted couplings between the source and the detector [1, Figure 1]. These are characterised by a leakage signal that bypasses the resonator and causes measured peaks to be asymmetric as a result of interference. Causes of the leakage signal include couplings between cables, and crosstalk between the loops/probes used to couple energy into a cavity resonator.
- The leakage signal is assumed not to vary significantly with frequency in practice a realistic assumption for typical measurements at RF and microwave frequencies (especially if the Q-factor is high). The effect of leakage that has a clearly delineated slope can be reduced by subtracting it from measurements if an experiment that can estimate the leakage is possible.
- The underlying shape of resonances measured in an ideal system (without a leakage signal) is assumed to be Lorentzian leakage is the only phenomenon that causes peaks to be asymmetric.
- Measured resonances are assumed to be spectrally-isolated from other resonances. Overlapping resonances are considered in reference [1, Section 4.5].
- The magnitude of the leakage signal is assumed to be smaller than the magnitude of the resonant peak.
- The work is aimed at measurement systems that record the magnitude of the transmission coefficient,  $|S_{21}|$ . The fitting algorithms can be applied when power is measured (e.g. with a thermal detector), but the effects of noise on systems with amplitude and power detectors are likely to be different (see Section 7.2).
- The response of the detection system is assumed to be linear so there is no *compression* at resonant peaks [1, Section 4.6]).
- In most cases,  $Q_L$  can be obtained from uncalibrated  $|S_{21}|$  data without a significant loss of accuracy.
- For weak-coupling, it is often sufficient to assume that  $Q_o \approx Q_L$ . If this is not the case, estimation of  $Q_o$  requires a scalar normalisation factor to be determined if the  $|S_{21}|$  data is uncalibrated or if there are attenuating *uncalibrated lines* (see Figure 1). Refer to Section 6 and reference [1] for more discussion.
- The source has a narrow linewidth in comparison to the resonance width (otherwise the shape of the resonance would be governed by a *convolution*).

#### 3 THEORY

The vector transmission coefficient of a resonator as a function of frequency f can be obtained from an equivalent circuit model [1, 2]. For a high Q-factor resonance ( $Q_L \gtrsim 100$ ), this yields a bilinear transform

$$S(f) = S_D + d \frac{e^{j\theta}}{1 + jQ_L t},$$
circuit (1)

in which the fractional offset frequency t is given by

$$t = 2\frac{f - f_L}{f_L}. (2)$$

 $S_D$  is a complex number that represents leakage signals that bypass the resonator, and d is the diameter of the Q-circle. The angle  $\theta$  defines the orientation of the Q-circle.

For measurements made by using a calibrated vector instrument,

$$S(f) = \alpha(f) e^{-j\phi} e^{-j\Delta\phi} \left[ S_D + d \frac{e^{j\theta}}{1 + jQ_L t} \right] + \text{imperfections} + \text{random noise.}$$
 (3)

The term  $\alpha(f)$  is a real valued quantity that describes attenuation in the uncalibrated lines. The terms  $\phi$  and  $\Delta\phi$  represent a constant and a frequency-dependent phase delay associated with cable connections ( $uncalibrated\ lines$ ).  $\Delta\phi$  can be significant for vector measurements because it causes change in the shape of Q-circles. NPL report MAT 58 [1] discusses methods of accounting for uncalibrated lines for vector measurements where necessary. One advantage of scalar measurement is that phase delay caused by uncalibrated lines need not be considered.

The *imperfections* term is included because the resonance (neglecting leakage) may not be Lorentzian. To proceed further, this possibility must be neglected. In this analysis, it is also assumed that  $S_D$  is constant in the measured frequency range.

The  $random\ noise$  is a complex quantity that represents nonrepeatability of data measured by the detection system (i.e. the receivers of a VNA). This gives rise to the noise floor of scalar measurements of |S(f)|. It is important to note that the random noise and the leakage vector are not separable quantities.

In most experiments, measurements on transmission resonators can be made with uncalibrated instruments because mismatches have very little effect [1]. The lack of scaling of uncalibrated measurements is not significant for determinations of  $Q_L$  (but does become important if unloaded Q-factor  $Q_o$  is required — see Section 6). A model-equation which allows for unscaled data can be obtained from equation (3) by introducing new real-valued coefficients  $b_1$ ,  $b_2$ ,  $c_1$  and  $c_2$ :

$$S(f) = \frac{b_1 + j b_2 + c_1 Q_L t + j c_2 Q_L t}{1 + j Q_L t}.$$
 (4)

After some manipulation, real and imaginary parts can be separated. These are

$$S' = \frac{b_1 + c_1 Q_L t + b_2 Q_L t + c_2 (Q_L t)^2}{1 + (Q_L t)^2}$$
 (5)

and

 $S'' = \frac{b_2 + c_2 Q_L t - b_2 Q_L t - c_1 (Q_L t)^2}{1 + (Q_L t)^2}.$  (6)

•

The transmitted power is given by

$$P = |S|^2 = (S')^2 + (S'')^2 \tag{7}$$

which is

$$P = \frac{\left(1 + (Q_L t)^2\right)}{\left(1 + (Q_L t)^2\right)^2} \left[b_1^2 + b_2^2 + 2b_1 c_1 Q_L t + 2b_2 c_2 Q_L t + c_1^2 (Q_L t)^2 + c_2^2 (Q_L t)^2\right]. \tag{8}$$

For convenience new coefficients  $m_0$ ,  $m_1$  and  $m_2$  are introduced to enable equation (8) to be written in the simpler form,

$$P = \frac{m_0 + m_1 Q_L t + m_2 (Q_L t)^2}{1 + (Q_L t)^2}.$$
 (9)

Thus, five coefficients ( $m_0, m_1, m_2, Q_L$  and  $f_L$ ) are sufficient to describe a scalar measurement on a resonance. Note that some of the terms contain products of coefficients (e.g.  $m_1Q_L$ ). If the leakage and noise floor have negligible effect,  $m_1 = m_2 = 0$  and so equation (9) reduces to the Lorentzian,

$$P = \frac{P_0}{1 + (Q_I t)^2},\tag{10}$$

where the peak power  $P_0 \equiv m_0$ .

#### 4 ROBINSON & CLEGG'S 3-COEFFICIENT SOLUTION

The solution by Robinson and Clegg [3] was originally developed for measuring the Q-factor of resonances of stirred-mode chambers that are used for measurements of Electromagnetic Compatibility (EMC). Their method solves equation (10) for  $f_L$ ,  $Q_L$  and  $m_0$ . Leakage and the noise floor are assumed to be small enough to neglect which, for the intended application, is often the case as power levels are high.

$$\frac{1}{P} = \frac{1}{m_0} \left( 1 + 4Q_L^2 \left( \frac{f^2}{f_L^2} - 2\frac{f}{f_L} + 1 \right) \right) \tag{11}$$

or

$$\frac{1}{P} = af^2 + bf + c \tag{12}$$

where

$$a = \frac{1}{m_0} \frac{4Q_L^2}{f_L^2} \tag{13}$$

$$b = -\frac{1}{m_0} \frac{8Q_L^2}{f_L} \tag{14}$$

and

$$c = \frac{1}{m_0} (4Q_L^2 + 1). {15}$$

The coefficients a, b and c can be obtained by using a polynomial fit. This yields

$$f_L = -\frac{b}{2a}. (16)$$

At the peak  $f = f_L$ , so  $m_0$  is related to  $Q_L$  by

$$m_0 = -\frac{8Q_L^2}{bf_L} = \frac{16 a Q_L^2}{b^2}.$$
 (17)

A solution for  $Q_L$  is obtained by substituting for  $m_0$ , giving the expression

$$c = \frac{b^2}{16 \, a \, Q_L^2} (4 Q_L^2 + 1). \tag{18}$$

Therefore

$$Q_L = \left(\frac{4ac}{b^2} - 1\right)^{-\frac{1}{2}}. (19)$$

Similarly,  $m_0$  is given by

$$m_0 = \left(c - \frac{b^2}{4a}\right)^{-1}. (20)$$

Listing 1 shows how Robinson and Clegg's method can be implemented in Python. A polynomial fitting routine to obtain a,b and c. The accuracy of this method for symmetric resonances is tested in simulations presented in Section 7.2. For typical measurements spanning a 3 dB width (frequency range  $f_L \pm 0.5 \, f_L/Q_L$ ), the best results are obtained when the data is unweighted. For the purpose of obtaining estimates of  $Q_L$  and  $f_L$  for asymmetric resonances, however, it is found to be beneficial to weight the data in proportion to P.

#### 5 ITERATIVE 5-COEFFICIENT SOLUTION

Resonances that are asymmetric as a result of leakage, or subject to a noise floor, are described by equation (9). The five coefficients can be obtained by iteration provided that estimates (termed *initial values* or *seed values*) are available. Convergence on the correct solution requires that these are reasonably close to the true values.

The first step is to obtain estimates of  $f_L$  and  $Q_L$ . The simplest approach is to estimate these from the peak maximum and 3 dB points, which can be found from the swept data by making searches. The built-in Lorentzian model in Python package LMFIT [6] uses this technique. The approach adopted here is to use Robinson and Clegg's polynomial-fitting method (Listing 1). The estimates are not very accurate for resonances that are asymmetric or have a high noise floor, but they are still useful as initial values. Simulations show that using the power data as weighting factors for the polynomial fit improves the robustness of the iterative solution that follows.

The second step is obtain initial values for  $m_0$ ,  $m_1$  and  $m_2$ . It is often sufficient to use  $m_0 = \max(P)$  and assume  $m_1 = m_2 = 0$ , but closer estimates can be obtained by using another polynomial fit (Listing 2). This requires x and y in equation (21) to be calculated at each measured frequency according to the estimates of  $f_L$  and  $Q_L$ :

$$x = Q_L t$$

$$y = P(1 + x^2)$$

$$y \approx m_0 + m_1 x + m_2 x^2 \Big|_{\text{Fit}}.$$
(21)

The third step is a weighted least-squares fit of the five coefficients to minimise the sum-squared residual error, given by:

$$RSS = \sum_{i} W_i \left( P_i - \overline{P}_i \right)^2. \tag{22}$$

where  $P_i$  and  $W_i$  are the measured power and weighting at the ith frequency in the sweep, and  $\overline{P}_i \equiv P\left(m_0, m_1, m_2, Q_L, f_L, f_i\right)$  calculated by using equation (9).

The author has used the curve\_fit and least\_squares functions from the scipy package to fit Q-factor, in both cases selecting the Levenberg-Marquardt algorithm. Identical results are obtained, but there are differences in the required coding. This is because the curve\_fit function allows pre-calculated weighting factors (specified by the input parameter  $\sigma = W^{-0.5}$ ) while the least\_squares function requires that the weighting factors are incorporated in the minimised function. This can be an advantage as they can be updated continually.

The least\_squares function (Listing 3) requires the residual error to be defined by the weighted differences as follows:

ResidErr 
$$(P, \overline{P}, W) = \sqrt{W}(P - \overline{P})$$
. (23)

**Listing 1:** Robinson and Clegg's method of solution (modified to use optional weightings).

```
from numpy.polynomial import polynomial
# Data: F is a numpy of frequency data.
        P is a numpy array of power data.
RP = 1.0/P
              # Weighting factors if required.
#W = None
W = P
              # Recommend using weightings when used to
              # generate initial values for iterative
              # solution for asymmetric peaks (Listing 3).
fit = polynomial.polyfit(F, RP, deg=2, w=W)
c, b, a = fit
tmp = 4*a*c/(b*b)
assert tmp>1.0, 'Failed_(leakage_too_large?)'
QL = 0.5/math.sqrt(tmp - 1.0) # QL and FL are used as initial values
                               # for iterative solution.
FL = -0.5*b/a
m0 = 1.0/(c-b*b/(4*a))
```

#### **Listing 2:** Obtain all five initial values (array XA) for iterative solution.

```
# Method 1: Polynomial fit
from numpy.polynomial import polynomial

x = 2.0*QL*(F/FL - 1.0)
y = P*(1.0 + x**2)
fit = polynomial.polyfit(x, y, deg=2)
m0, m1, m2 = fit

XA = m0, m1, m2, FL, Q

# Method 2: assume m1 = m2 = 0
# XA = max(P), 0.0, 0.0, FL, QL
```

To calculate the weighting factors, the Jacobian matrix, and the residual error, requires additional computer code which is described below.

**Weighting factors** Q-factor is defined at resonance, so it would appear natural to apply a reduced weighting for data which is not close to the resonant frequency. Closer investigation shows that for scalar fitting measurements by amplitude detection (e.g. using a VNA), it is often better to apply no weightings (see Section 7.2 for more discussion). The code listings give a few options which are chosen by using input parameter WeightMode.

WeightMode = 0 The data is not weighted (normally recommended).

**Listing 3:** Iterative solution by using a library function (least squares).

WeightMode = 1 The data is weighted in proportion to power for an equivalent pure Lorentzian (i.e.  $m_1$  and  $m_2$  are disregarded). The weighting factor at the ith frequency is given by

$$W_{i} = \frac{1}{1 + \left[\frac{2Q_{L}(f_{i} - f_{L})}{f_{L}}\right]^{2}} . \tag{24}$$

The same weighting formula is derived in reference [1, equation (28)] for fitting in the complex domain.

WeightMode = 2 An array of pre-calculated weighting factors is used.

**Scaling** The fitted coefficients can differ by many orders of magnitude. The input parameter x\_scale is a list of values for normalising the fitted coefficients so that they all have similar magnitude. If this is omitted, the fitting process may terminate without finding the optimum solution.

**Jacobian matrix** This is the name used for a matrix of partial differentials that can be provided to improve efficiency (Listing 4). It also makes the fitting process more robust. Note that the partial differentials must be multiplied by the square root of the weighting factors when fitting is performed using the least\_squares function in the scipy package.

**Residual error function** The difference between measured data *P* and the values calculated for current estimate for coefficients (Listing 5). Note that this must be multiplied by the square root of the weighting factors when fitting is performed using the least\_squares function in the scipy package.

#### **Listing 4:** Function for calculating the Jacobian matrix (weighted).

```
def Jacobian5(X, F, P, WeightMode, SqrtWtArray):
   m0, m1, m2, FL, QL = X
    Jac = np.zeros([len(F),5])
    t = 2.0*(F/FL - 1.0)
    qt = QL^*t
    qt2 = qt**2
    den = 1.0 + qt2
    den2 = den**2
    d dm0 = 1.0/den
    d dm1 = qt/den
    d_dm2 = qt2/den
    v = m2*qt2 + m1*qt + m0
    d_dF = (-4.0*QL*F*m2*qt/FL**2 - 2.0*QL*F*m1/FL**2)/den 
           + 4.0*QL*F*qt*v/(FL**2*den2)
    d_dq = -2.0*qt*t * v/den2 + (2.0*qt*m2*t + m1*t)/den
    if not WeightMode: RootW = 1.0
    elif WeightMode==1: RootW = np.sqrt(1.0/(1.0+qt2))
    elif WeightMode==2: RootW = SqrtWtArray
    Jac[:,0] = RootW*d_dm0
    Jac[:,1] = RootW*d_dm1
    Jac[:,2] = RootW*d_dm2
    Jac[:,3] = RootW*d_dF
    Jac[:,4] = RootW*d_dq
return Jac
```

#### **Listing 5:** Function for calculating the residual error (weighted).

```
def Fun5(X, F, P, WeightMode, SqrtWtArray):
    m0, m1, m2, FL, QL = X
    qt = 2.0*QL*(F/FL - 1.0)
    qt2 = qt**2
    if not WeightMode: RootW = 1.0
    elif WeightMode==1: RootW = np.sqrt(1.0/(1.0+qt2))
    elif WeightMode==2: RootW = SqrtWtArray
    pfit = (m0 + m1*qt + m2*qt2)/(1.0+qt2)
    Resid = (pfit -P)*RootW
return Resid
```

#### **6 ESTIMATION OF UNLOADED Q-FACTOR**

If the coupling factors at the two ports are similar, unloaded Q-factor can be estimated from the calibrated Q-circle diameter d of the  $S_{21}$  Q-circle by using a simple formula [1],

$$Q_o = \frac{Q_L}{1 - d} \quad . \tag{25}$$

For weak coupling (e.g.  $d \approx 0.01$ ) it may be sufficient to assume that  $Q_o \approx Q_L$ .

It is usually the case that the fitted coefficients are determined from uncalibrated measurements of  $|S_{21}|$ . To obtain d therefore requires a normalisation factor to be determined. This can be obtained by measuring the magnitude at "full-scale deflection" (FSD) when the resonator is replaced by a through connection [1]. This measurement should be made at approximately the resonant frequency. It is convenient to define a scaling factor A=1/FSD. For measurements in a calibrated system in which the uncalibrated lines are non-attenuating, A=1.

For vector measurements, the d is provided directly by the fitting process [1]. For scalar measurements, a calculation is needed when there is leakage. The frequencies at the minimum and maximum power levels are found by differentiating equation (9) and solving for frequency (it may be helpful to refer to Figure 2). The diff and solve functions in the Python sympy package can be used to assist these derivations.

$$f_{\min} = \frac{f_L(m_2 - m_0) + 2f_L Q_L m_1 - f_L \sqrt{m_0^2 + m_1^2 + m_2^2 - 2m_0 m_2}}{2Q_L m_1}$$
(26)

$$f_{\text{max}} = \frac{f_L(m_2 - m_0) + 2f_L Q_L m_1 + f_L \sqrt{m_0^2 + m_1^2 + m_2^2 - 2m_0 m_2}}{2Q_L m_1}$$
(27)

From equations (26) and (27) the minimum  $(p_{\text{max}})$  and maximum  $(p_{\text{min}})$  power levels can be calculated by using equation (9). They could be in either order. Two differing solutions for the calibrated Q-circle diameter are obtained when there is a leakage signal:

$$d = A\left(\sqrt{P_{\text{max}}} \pm \sqrt{P_{\text{min}}}\right). \tag{28}$$

Consequently, there are two possible solutions for  $Q_o$  — see Section 7.3 for further discussion and an example.

If the leakage is negligible (i.e.  $m_1/m_0 \approx 0$  and  $m_2/m_0 \approx 0$ ) the pole of the resonance is located at the origin of the polar chart (so  $p_{\min} \approx 0$ ). Moreover, the maximum power occurs at frequency  $f_{\max} \approx f_L$  and there is a unique solution for Qo.

Listing 6 shows a Python implementation of the calculation of  $Q_o$  from a scalar fit by using the equations above.

**Listing 6:** Calculation of unloaded Q-factor from the fitted  $m_0, m_1, m_2, f_L$  and  $Q_L$ .

```
QCircleDia1 = QCircleDia2 = Qo1 = Qo2 = None
CorrQCircleDia1 = CorrQCircleDia2 = None
MagLeak = 0.0
if abs(m1/m0)+abs(m2/m0)>1.0e-6:
    f1 = FL*(m2-m0 + 2.0*QL*m1 + math.sqrt((m2-m0)**2 + m1**2))/(2*QL*m1)
    f2 = FL^*(m2-m0 + 2.0*QL*m1 - math.sqrt((m2-m0)**2 + m1**2))/(2*QL*m1)
   p1 = Power(f1, X)
   p2 = Power(f2, X)
    if p1>p2: tmp=p1; p1=p2; p2=tmp
    if p1 < 0.0:
        print('Minimum_power_negative._Assuming_this_is_a_rounding_error')
    else:
        MagLeak = math.sqrt(p1)
    if p2 > 0.0:
        QCircleDia1 = math.sqrt(p2)-MagLeak
        QCircleDia2 = math.sqrt(p2)+MagLeak
        CorrQCircleDia1 = A*QCircleDia1
        Qo1 = QL/(1.0-CorrQCircleDia1)
        CorrQCircleDia2 = A*QCircleDia2
        Qo2 = QL/(1.0 - CorrQCircleDia2)
        print('Corrected_Q-circle_diameters_(two_solutions)',
              CorrQCircleDia1 , CorrQCircleDia2 )
        print('Unloaded_Q-factors',Qo1,Qo2)
    else:
        print('Power_fitted_at_peak_negative_-_cannot_get_unloaded_Q')
else:
    p1 = Power(FL, X)
    QCircleDia1 = math.sqrt(p1)
    CorrQCircleDia1 = A*QCircleDia1
    Qo1 = QL/(1.0 - CorrQCircleDia1)
    print('Corrected_Q-circle_diameter_(one_solution)',CorrQCircleDia1)
    print('Unloaded_Q-factor',Qo1)
```

#### 7 TESTS

Table 1 lists fitting methods that are tested. In three tests, Q-factors fitted by these methods to measured and simulated data are compared.

<b>Table 1:</b> Q-factor fitting methods that are investigat
--

Algorithm	No. of fitted coefficients	Туре	Comments
NLQFIT6	6	Vector	Documented in references [1] and [2].
ROBINSON	3	Scalar	As Listing 1. Optional weighting-factors (W).
SCALARQFIT3	3	Scalar	Lorentzian (fits equation (10) to data).
SCALARQFIT5	5	Scalar	Asymmetric peak (fits equation (9) to data).  Code in Listings 1 to 6.

# 7.1 TEST 1: FITTING-METHOD COMPARISON FOR WELL-SHAPED EXPERIMENTAL DATA

A swept measurement of the complex transmission-coefficient  $(S_{21})$  of Split-Post Dielectric Resonator (SPDR) is used for this test. The data has been published previously in reference [1, Figure 6(b)]. The measured mode (quasi-TE01 $\delta$ ) is a well-shaped Lorentzian with low leakage. Moreover, the noise floor of the data measured by the VNA (Agilent 8753ES) is very low — approximately 50 dB below the peak of the resonance. Very good agreement between the algorithms and measured data is obtained (Table 2 and Figure 3). For this almost ideal data, Robinson and Clegg's method [3], which requires only a few lines of computer code, is observed to have similar accuracy to the other methods. The frequency range of the data is  $f_L \pm f_L/Q_L$ .

For this set of data, the fit obtained by using SCALARQFIT5 has a minor anomaly: the minimum of the fitted power (at the pole of the resonance) is negative, albeit by a very small amount. This occurs because the shape of the resonance is not quite perfect and the leakage is very low. To avoid a runtime error when calculating the Q-circle diameter d by using equation (28), the power at the pole (Listing 6) is rounded to zero. Therefore, the two solutions for  $Q_o$  are identical. An alternative tactic is to repeat the fit with a small offset added to the  $S_{21}$  amplitude data.

Table 2: Vector and scalar fits for a measurement on a Split-Post Dielectric Resonator (SPDR)

Algorithm	Weightings	$Q_{\mathrm{L}}$	* d (calibrated)	$Q_{o}$
NLQFIT6	[1, Eqn. (28)]	7454	0.0121	7546
ROBINSON	None	7458	†0.0120	7548
SCALARQFIT3	None	7451	†0.0120	7542
SCALARQFIT5	None	7444	‡0.0120	<b>‡</b> 7534
SCALARQITIS	None	7444	‡0.0120	<b>‡</b> 7534

<sup>\*</sup> The fitted diameter of the  $S_{21}$  Q-circle normalised to a "thru" measurement.

<sup>†</sup>The square root of the fitted peak power.

<sup>‡</sup> Calculated by using equation (28). The solutions are identical — see text for explanation.

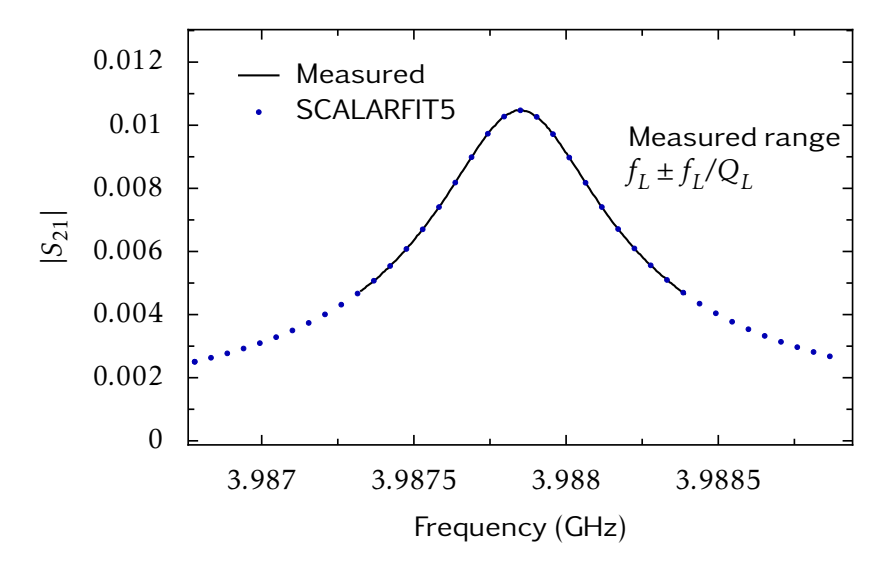


**Figure 3:** Fitted resonance of a Split-Post Dielectric Resonator (magnitude vs. frequency).

# 7.2 TEST 2: COMPARISON OF VECTOR AND SCALAR FITS TO SIMULATED DATA WITH NOISE BUT NO LEAKAGE

Tests were made using simulated VNA transmission measurements with independent noise on both real and imaginary receivers at each point in the frequency sweep of 201 points. The leakage signal is specified as zero. Computer code for creating the data is shown in Listing 7. Q-factors were obtained by vector and scalar methods for 10 000 trials. Figures 4a and 4b show one trial. The following comparisons were made:

- From the complex  $S_{21}$  data by performing weighted fits by using NLQFIT6 [1]. As noted previously, fitting in the complex domain provides reliable solution even when the VNA receiver-noise is high [2, Figure 5]. The weightings used are calculated according to the Lorentzian formula see reference [1, Section 2.4] for more information.
- From the measured power  $|S_{21}|^2$  by performing scalar fits by using ROBINSON. The data is weighted by the measured power (W=P in Listing 1).
- From the measured power  $|S_{21}|^2$  by performing scalar fits by using ROBINSON. No weightings are used, as in the original paper [3] (W=None in Listing 1).
- From the measured power  $|S_{21}|^2$  by performing scalar fits by using SCALARQFIT5. The data is weighted in proportion to the power calculated from the  $f_L$  and  $Q_L$  obtained in the previous iteration according to the Lorentzian formula, i.e.  $W_i = 1/\left(1.0 + \left(Q_L t_i\right)^2\right)$  (WeightMode=1 in Listings 3 5).
- From the measured power  $|S_{21}|^2$  by performing scalar fits by using SCALARQFIT5. No weightings<sup>3</sup> are used during the iterative solution (WeightMode=0 in Listings 3 5).

The above calculations were carried out for three frequency ranges:  $f_L \pm 2f_L/Q_L$ ,  $f_L \pm f_L/Q_L$  and  $f_L \pm 0.5f_L/Q_L$ . The data obtained is plotted as histograms in Figures 4c and 5. The standard deviations of Q-factors obtained from the simulations are shown in Table 3.

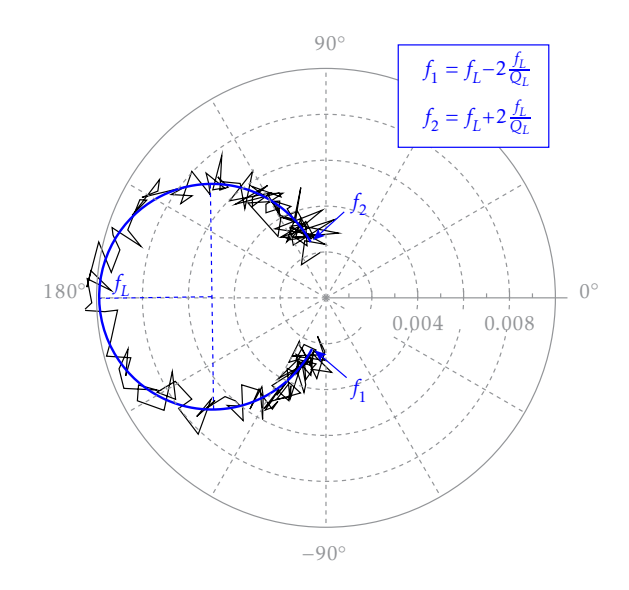
<sup>&</sup>lt;sup>3</sup> SCALARQFIT5 always applies weightings during the calculation of initial values (Listing 1).

**Listing 7:** Function for generating trial  $S_{21}$  data with VNA receiver noise.

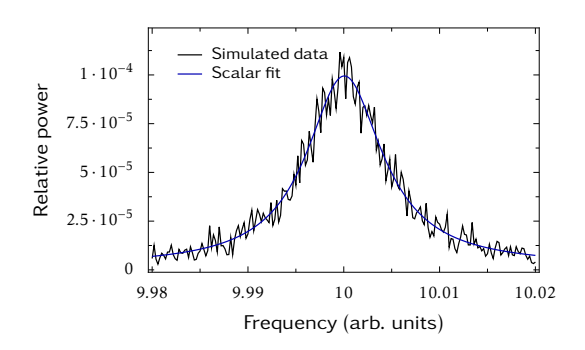
```
import random
# Data
FL = 10.0
                            # Resonant frequency in arbitrary units
QL = 1000.0
                            # Loaded Q-factor
gamma_s = complex(0.0,0.0) # Leakage vector (no leakage)
d = 0.01
                            # Q-circle diameter
noise = 0.0005
                            # random noise, normal distribution
# Function
def model_gamma(gamma_s, d, QL, deltaF, FL, noise):
    g = gamma_s + d*exp(complex(0.0,pi))/complex(1.0, 2.0*QL*deltaF/FL)
    return complex(random.normalvariate(g.real, noise), \
                   random.normalvariate(g.imag, noise))
# Note: deltaF = Frequency - FL
```

#### Several observations can be made:

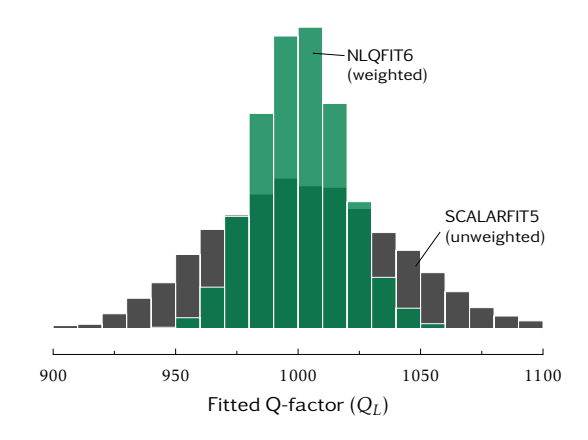
- The simulated amplitude noise on VNA receivers results in power noise that is greatest at peaks (Figure 4b). Noise associated with other types of instrumentation, e.g. ones that use direct measurement of power, may not show this behaviour.
- At higher noise-levels NLQFIT6 is the most robust of the methods tested (see also reference [2, Section IV]).
- When the standard deviation of the noise  $\gtrsim 10\%$  of the Q-circle diameter, SCALARQFIT5 can find the wrong least-squares minimum, or not converge on a solution at all.
- The standard deviation of the mean of the 10 000 trials ( $\sigma/100$ ) and the average  $Q_L$  are consistent to within 0.1% of the defined value  $Q_L=1000$  for simulations fitted by using NLQFIT6. None of the scalar methods offer such good consistency, although several of them are consistent to within better than 1%.
- For weighted fits to a wide sweep (Figure 5a and Table 3), ROBINSON produces rather low values of  $Q_L$ . In other words, the simulated noise makes the fitted peak appear broader.
- Unweighted fits to a wide sweep made by using ROBINSON showed a large variation in fitted Q-factors (Figure 5a) and sometimes exited with an error (tmp ≤ 1.0 in Listing 1). The SCALARFIT5 algorithm applies weights for the calculation of initial values using ROBINSON because this improves the likelihood of convergence on the correct solution.
- For fitting Q-factors to data with simulated receiver noise, ROBINSON gives its best repeatability for a narrow sweep, whereas SCALARQFIT5 gives its best repeatability for a wide sweep. This is because the ROBINSON model is fitted to 1/P, whereas the SCALARQFIT5 is fitted to P. For fits obtained by using SCALARQFIT5, this can lead to a dilemma because  $Q_L$  is defined at resonance and, in the absence of noise, the best adherence of experimental data to the Lorentzian shape is usually near the peak. In other words, an experimentalist would normally prefer to use a narrow sweep range.



(a): Trial  $S_{21}$  for a broad sweep plotted on a polar chart.

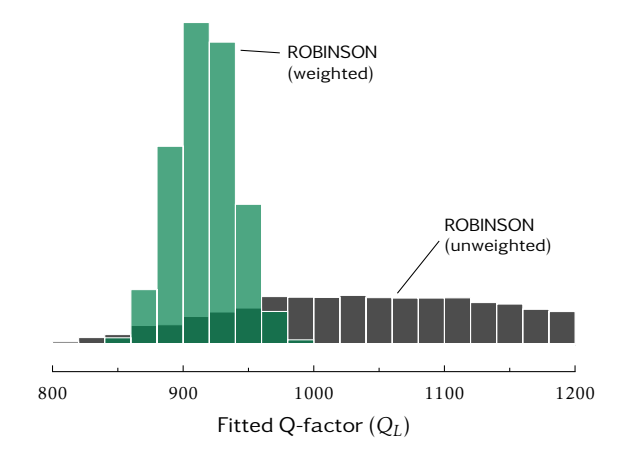


(b): Trial  $S_{21}$  plotted as relative power ( $\left|S_{21}\right|^2$ ).

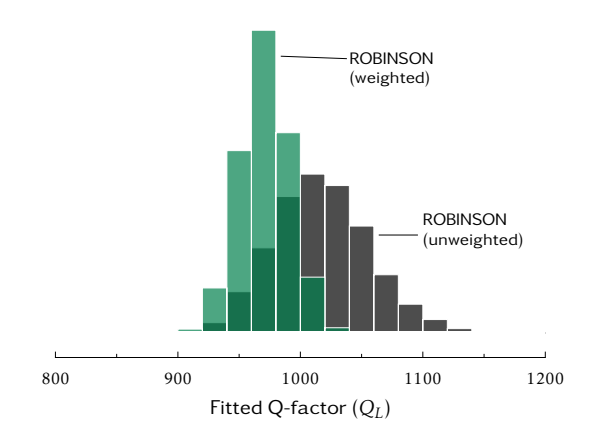


(c): Histogram created from 10000 trials.

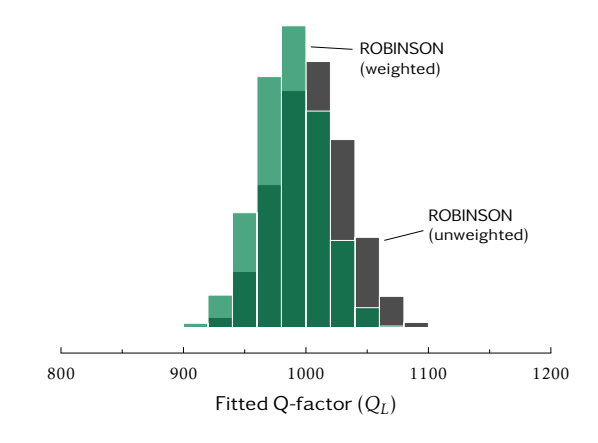
**Figure 4:** Simulated data with VNA receiver noise. Computer code for generating the data is shown in Listing 7. The nominal value of  $Q_L$  is 1000. The simulations used 201 swept frequencies. The frequency range was  $f_L \pm 2f_L/Q_L$ .



(a): Sweep range  $f_L \pm 2 f_L/Q_L$ .



**(b):** Sweep range  $f_L \pm f_L/Q_L$ .



(c): Sweep range  $f_L \pm 0.5 f_L/Q_L$ .

**Figure 5:** Simulations of Q-factors fitted by ROBINSON plotted as histograms. Data is weighted by the simulated power where indicated. Computer code for generating the data is shown in Listing 7. The simulations used 201 swept frequencies for sweep ranges as shown. Some of the unweighted fits shown in (a) failed — in these cases fits to replacement trials were used.

**Table 3:** Results of simulations for a resonance with noise but no leakage. Computer code for generating the data is shown in Listing 7. There were 201 swept frequencies.

Algorithm	Span $f_L \pm 2 f_L/Q_L$	$\mathbf{Span} \; \mathbf{f}_{\mathrm{L}} \pm \mathbf{f}_{\mathrm{L}}/\mathbf{Q}_{\mathrm{L}}$	$\mathbf{Span} \; \mathbf{f}_{\mathrm{L}} \pm 0.5  \mathbf{f}_{\mathrm{L}} / \mathbf{Q}_{\mathrm{L}}$			
Aigurtiiii	$ extbf{Q}_{ ext{L}} \pm \sigma_{n-1}  ext{ from }  ext{10 000 trials}$					
NLQFIT6 (Weighted†)	$1001 \pm 18$	$1001 \pm 17$	$1001 \pm 24$			
ROBINSON (Weighted†)	$917 \pm 24$	$971 \pm 20$	$987 \pm 26$			
ROBINSON (Unweighted)	$1211 \pm 1011$	$1017 \pm 39$	$1005 \pm 30$			
SCALARQFIT5 (Weighted†)	$1009 \pm 53$	$1014 \pm 56$	$1065 \pm 116$			
SCALARQFIT5 (Unweighted)	$1003 \pm 38$	$1004 \pm 52$	$1010 \pm 153$			

†See page 15 for a description of the weighting scheme used for each algorithm.

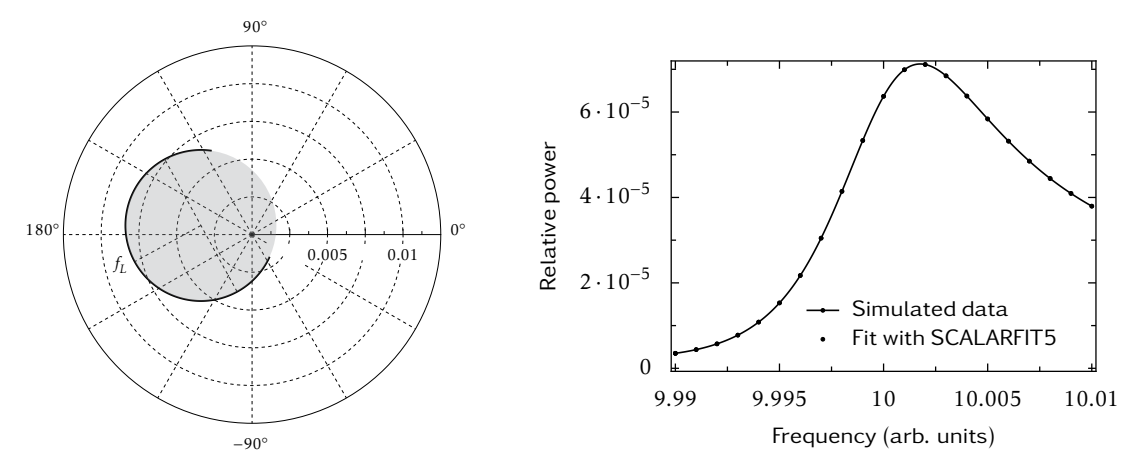
# 7.3 TEST 3: CALCULATIONS OF UNLOADED Q-FACTOR WHEN THERE IS LEAKAGE

To test the accuracy of Q-factors fitted by SCALARQFIT5, two sets of simulated data were created (Figure 6). These have different leakage vectors, but no simulated noise. The fitted results are shown in Table 4. For each set of data, one of the two solutions for  $Q_o$  has the correct value (1010.10), but it would not be possible to say which on the basis of one set of scalar data alone. The differences between  $Q_L$  and the solutions for  $Q_o$  for this example are quite small as the coupling is weak (so d is low-valued). Resonant circuits used in some applications (e.g. low-noise oscillators) require stronger coupling, in which case loaded and unloaded Q-factors may differ significantly.

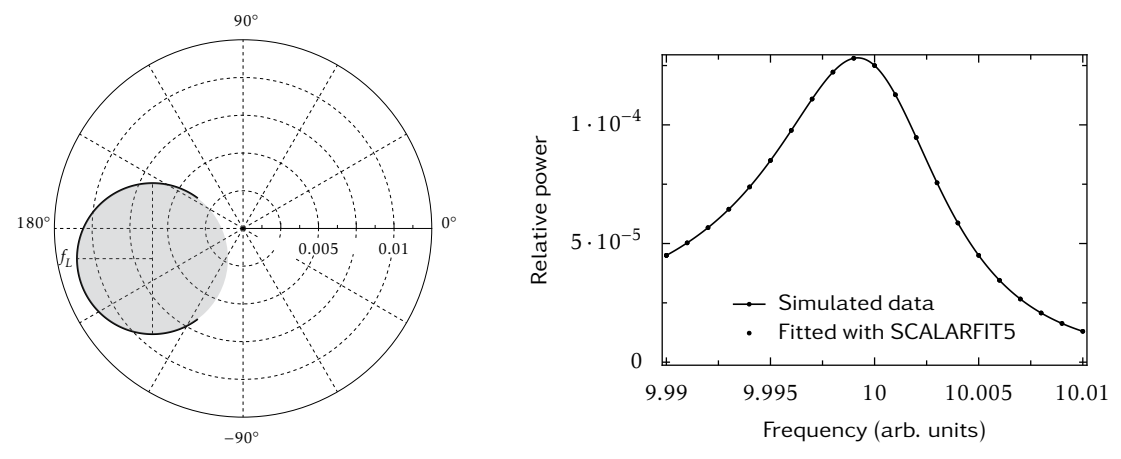
**Table 4:** Unloaded Q-factors obtained from the coefficients fitted by SCALARFIT5 by using equations (26) and (27).

	Simulated data		First solution		Second solution		
	d	$Q_L$	$^{\dagger}Q_{o}$	d	$Q_o$	d	$Q_o$
Figure 6a	0.0100	1000.00	1010.10	0.0069	1006.93	0.0100	1010.10
Figure 6b	0.0100	1000.00	1010.10	0.0100	1010.10	0.0126	1012.81

†Calculated by using equation (25).



(a): With the centre of the polar chart inside the Q-circle.



(b): With the centre of the polar chart outside the Q-circle.

**Figure 6:** Simulated resonances with leakage signal ( $Q_L$ =1000 and d = 0.01).

#### 8 CONCLUSION

In this report, formulae for describing the power transmission for scalar resonances have been derived. These apply to systems that measure amplitude, such as network analysers. Leakage, which has the effect of making resonant peaks asymmetric, is accounted for in a model equation that has five coefficients. Formulae for calculating the unloaded Q-factor  $Q_o$  of scalar measurements have also been derived. It is found that when the leakage is non-zero, the calculated unloaded Q-factor is ambiguous as it has two solutions. Scalar fitting is not quite as accurate as vector fitting, nor as robust when used to fit noisy data. Nevertheless, good agreement between vector and scalar methods has been demonstrated.

Minimal implementations of computer code for iterative solution of the five coefficients have been tested against measured and simulated data. Estimates of the uncertainty of the fitted coefficients can be obtained from repeatability measurements. Alternatively, tools provided by the Python package LMFIT could be used for estimating uncertainty as a byproduct of each least-squares fit. If there are significant Type B contributions, as is often the case, experimental techniques may be needed to give realistic estimates of uncertainty [1].

#### **REFERENCES**

- [1] A. P. Gregory. *Q-factor measurement by using a Vector Network Analyser*. Tech. rep. MAT 58. National Physical Laboratory, Dec. 2021. url: https://doi.org/10.47120/npl.MAT58.
- [2] A. P. Gregory, P. D. Woolliams, and S. M. Hanham. "Robust Algorithms for Fitting Q-Factor in the Complex Domain". In: *IEEE Access* 12 (2024), pp. 188336–188348. ISSN: 2169-3536. URL: http://dx.doi.org/10.1109/ACCESS.2024.3514707.
- [3] M. P. Robinson and J. Clegg. "Improved Determination of Q-Factor and Resonant Frequency by a Quadratic Curve-Fitting Method". In: *IEEE Transactions on Electromagnetic Compatibility* 47.2 (May 2005), pp. 399–402. ISSN: 0018-9375. URL: http://dx.doi.org/10.1109/TEMC.2005.847411.
- [4] S. Mueller et al. "Characterization of an open resonator with low-permittivity thin films utilizing a frequency-comb locked continuous-wave terahertz spectrometer". In: *Submitted to IRMMW-THz 2025, Espoo, Finland*. IEEE, 2025.
- [5] D. M. Pozar. Microwave engineering; 4th ed. Hoboken, NJ: Wiley, 2012.
- [6] M. Newville et al. *LMFIT: Non-linear least-squares minimization and curve-fitting for Python, Version 1.2.2.* url: https://zenodo.org/records/12785036.
- [7] J. R. Bray and L. Roy. "Measuring the unloaded, loaded, and external quality factors of one- and two-port resonators using scattering-parameter magnitudes at fractional power levels". In: *IEE Proceedings Microwaves, Antennas and Propagation* 151.4 (2004), p. 345. URL: https://doi.org/10.1049/ip-map:20040521.
- [8] P. J. Petersan and S. M. Anlage. "Measurement of resonant frequency and quality factor of microwave resonators: Comparison of methods". In: *Journal of Applied Physics* 84.6 (Sept. 1998), pp. 3392–3402. URL: https://doi.org/10.1063/1.368498.
- [9] B. J. Zadler et al. "Resonant Ultrasound Spectroscopy: theory and application". In: *Geophysical Journal International* 156.1 (Jan. 2004), pp. 154–169. ISSN: 1365-246X. URL: http://dx.doi.org/10.1111/j.1365-246X.2004.02093.x.
- [10] G. V. Kuptsov, V. A. Petrov, and V. V. Petrov. "Algorithm for Determination of Resonance Lorentzian Curve Parameters". In: Bulletin of the Lebedev Physics Institute 50.S2 (Aug. 2023), S240–S249. ISSN: 1934-838X. URL: http://dx.doi.org/10.3103/S1068335623140099.